Eidgenössische
Technische Hochschule
Zürich

Ecole polytechnique fédérale de Zurich
Politecnico federale di Zurigo
Swiss Federal Institute of Technology Zurich

Finite volume methods for the two-fluid MHD equations

H. Kumar

Research Report No. 2010-29
September 2010

Seminar für Angewandte Mathematik
Eidgenössische Technische Hochschule
CH-8092 Zürich
Switzerland

Finite Volume Methods for the Two-fluid MHD Equations

Harish Kumar
E-mail: harish@math.ethz.ch
Seminar for Applied Mathematics,
ETH Zurich, CH-8092.

Abstract

Two fluid (TF) ideal magnetohydrodynamics (MHD) equations are a generalized form of the ideal MHD equations in which the electrons and ions are considered as separate species. The design of efficient numerical schemes for the these equations is complicated on account of the non-linearities and the presence of stiff source terms, particularly for realistic charge to mass ratios. We design novel finite volume schemes based on an implicit-explicit (IMEX) time stepping routine. The special structure of the two-fluid MHD equations enable us to split the source terms carefully in order to ensure that only local (in each cell) equations need to be solved at each time step. Furthermore, these equations are solved exactly. Benchmark numerical experiments are presented to illustrate the efficiency of new approach.

1 Introduction

Flows in plasmas are frequently modeled by the equations of ideal magnetohydrodynamics (MHD). These equations combine the Euler equations for compressible flow together with Maxwell's equations for magnetic fields. These equations assume *quasi-neutrality* i.e. the difference in number density of ions and electrons is ignored.

However, in many applications like fast magnetic reconnection, the assumption of quasi-neutrality is violated. In such cases, one resorts to extended MHD models for the plasmas. A popular example models the flow of two different species, one electron and one ion, separately. This result in the so-called two fluid MHD (TF-MHD) equations (see [1], [2]). In non-dimensional form, these equations are,

$$\frac{\partial \rho_i}{\partial t} + \nabla \cdot (\rho_i \vec{v}_i) = 0, \tag{1.1a}$$

$$\frac{\partial (\rho_i \vec{v}_i)}{\partial t} + \nabla \cdot \left(\rho_i \vec{v}_i \vec{v}_i^{\top} + p_i \mathbf{I}\right) = \frac{1}{\hat{r}_g} \rho_i (\vec{E} + \vec{v}_i \times \vec{B}), \tag{1.1b}$$

$$\frac{\partial E_i}{\partial t} + \nabla \cdot ((E_i + p_i)\vec{v}_i) = \frac{1}{\hat{r}_g}\rho_i(\vec{E} \cdot \vec{v}_i), \tag{1.1c}$$

$$\frac{\partial \rho_e}{\partial t} + \nabla \cdot (\rho_e \vec{v}_e) = 0, \tag{1.1d}$$

$$\frac{\partial (\rho_e \vec{v}_e)}{\partial t} + \nabla \cdot \left(\rho_e \vec{v}_e \vec{v}_e^{\top} + p_e \mathbf{I}\right) = -\frac{\lambda_m}{\hat{r}_g}\rho_e(\vec{E} + \vec{v}_e \times \vec{B}), \tag{1.1e}$$

$$\frac{\partial E_e}{\partial t} + \nabla \cdot ((E_e + p_e)\vec{v}_e) = -\frac{\lambda_m}{\hat{r}_g}\rho_e(\vec{E} \cdot \vec{v}_e), \tag{1.1f}$$

$$\frac{\partial \vec{B}}{\partial t} + \nabla \times \vec{E} + \kappa \nabla \psi = 0, \tag{1.1g}$$

$$\frac{\partial \vec{E}}{\partial t} - \hat{c}^2 \nabla \times \vec{B} + \xi \hat{c}^2 \nabla \phi = -\frac{1}{\hat{\lambda}_d^2 \hat{r}_g}(r_i \rho_i \vec{v}_i + r_e \rho_e \vec{v}_e), \tag{1.1h}$$

$$\frac{\partial \phi}{\partial t} + \xi \nabla \cdot \vec{E} = \frac{\xi}{\hat{\lambda}_d^2 \hat{r}_g}(r_i \rho_i + r_e \rho_e), \tag{1.1i}$$

$$\frac{\partial \psi}{\partial t} + \kappa \hat{c}^2 \nabla \cdot \vec{B} = 0. \tag{1.1j}$$

Here subscript $\{i, e\}$ refers to the ion and electron species respectively, $\rho_{\{i,e\}}$ are densities, $\vec{v}_{\{i,e\}} = (v^x_{\{i,e\}}, v^y_{\{i,e\}}, v^z_{\{i,e\}})$ are velocities, $E_{\{i,e\}}$ are the energies, $p_{\{i,e\}}$ are the pressures, $\vec{B} = (B^x, B^y, B^z)$ is magnetic field, $\vec{E} = (E^x, E^y, E^z)$ is electric field, ϕ, ψ are the potentials and ξ, κ are the speeds for Maxwell's equations. Also $r_i = \frac{q_i}{m_i}$ and $r_e = \frac{q_e}{m_e}$ are charge to mass ratios of ions and electrons respectively.

The Eqns. (1.1a)-(1.1c) represent the conservation of mass, momentum and energy for the ions. The source term in (1.1b) represents the Lorentz force acting on ions due to the electric and magnetic fields. Similarly Eqns.(1.1d)-(1.1f) represent conservation of these quantities for electrons. Eqns. (1.1g)-(1.1j) are the perfectly hyperbolic Maxwell's (PHM) equations (see [4]). These equations satisfy the divergence free condition approximately, and are consistent with the hyperbolic structure of the fluid equations. In addition we assume that both ions and electrons satisfy ideal gas law with gas constant $\gamma = \frac{5}{3}$.

Many physically significant parameters appear in the non dimensionalized form of the TF equations. Here, $\hat{r}_g = \frac{m_i v_i^T}{q_i B_0 x_0}$ is the normalized ion Larmor radius, $\lambda_m = m_i/m_e$ is the ion-electron mass ratio, $\hat{c} = c/v_i^T$ is the normalized speed of light and $\hat{\lambda}_d = \lambda_d / r_g$ is the ion Debye length normalized with Larmor radius. Also v_i^T is the reference thermal velocity of ions, B_0 is the reference magnetic field and x_0 is the reference length. Ion mass m_i is assumed to be 1. Note that when Larmor radius $\hat{r}_g \to 0$, the TF model approaches the MHD limit. Similarly for $\hat{r}_g \to \infty$ (1.1) reduce to simple flow (Euler) equations for ions and electrons. TF

equations model the intermediate physics between these two limits.

For simplicity, we will focus on the TF equations in one space dimension for the rest of this paper. Eqns. (1.1) can be written as a system of balance laws,

$$\mathbf{U}_t + \mathbf{F}(\mathbf{U})_x = \mathbf{S}(\mathbf{U}). \tag{1.2}$$

Here the vector of unknowns $\mathbf{U}$, the flux vector $\mathbf{F}$ and the source vector $\mathbf{S}$ can be read from (1.1). It is well known that solutions of (1.2) consist of discontinuities in the form of shocks and contact discontinuities. Numerical algorithms have to take into account the formation of these complex waves and their interactions. Finite volume methods (FVM) have been quite successful in approximating balance laws of the form (1.2) (see [3]). In particular, one has to device suitable numerical flux functions in order to approximate these waves.

However, the most challenging issue in designing efficient algorithms for (1.1) is the stiffness of the source terms. As an example, consider a generic situation involving a mass ratio of 1832.6, non-dimensonal Debye length of 0.01, and Larmor radius of 0.005. Assuming that all the other quantities are of $O(1)$, the strength of source term is 3.6652×10^9. Thus, explicit time stepping will be extremely expensive computationally due to small time steps.

The TF equations have received some attention in recent years. In [1], the authors used a second order operator splitting approach and a fourth order Runge-Kutta (RK4) method to discretize source terms in time. This approach is easy to implement but computationally expensive. In [2], the authors treat source terms implicitly and flux terms explicitly. The resulting equations are solved using Newton iterations. This method might be diffusive and may require many iterations for each time step.

In this paper, we propose a novel implicit-explicit(IMEX) scheme to discretize (1.1) based on the following ingredients:

1. The numerical fluxes are designed by exploiting the split structure of the flux in (1.1) and are integrated in time explicitly.
2. The source terms are treated implicitly. We observe and exploit the special structure of the source terms in order to device an implicit scheme that requires solving cell-wise linear system of equations. The local mass matrices are inverted symbolically and are evaluated at each time step.
3. High order spatial accuracy is obtained by non-oscillatory piecewise linear reconstruction in each cell. High order time integration is performed using SSP-RK methods (see [5]).

Rest of the paper is organized as follows: In Section 2, we describe the proposed IMEX algorithm. In Section 3, we present the numerical results for two numerical test examples.

2 Finite Volume Methods

Consider a computational domain $(0, L)$ (for some $L > 0$), discretized uniformly(for simplicity), with mesh size Δx in to cells $[x_{i-\frac{1}{2}}, x_{i+\frac{1}{2}}]$. We aim to approximate the cell averages $\mathbf{U}_i^n \approx \frac{1}{\Delta x}\int_{x_{i-\frac{1}{2}}}^{x_{i+\frac{1}{2}}} \mathbf{U}(x, t^n)dx$ at time level t^n. Denote the time-step Δt^n at time level t^n, then a first order IMEX scheme for (1.1) is written as

$$\frac{\mathbf{U}_i^{n+1} - \mathbf{U}_i^n}{\Delta t} = -\frac{1}{\Delta x}\left(\mathbf{F}^n_{i+\frac{1}{2}} - \mathbf{F}^n_{i-\frac{1}{2}}\right) + \mathbf{S}(\mathbf{U}_i^{n+1}). \tag{2.1}$$

2.1 Numerical flux function

Denote $\mathbf{U} = \{\mathbf{U}^f, \mathbf{U}^m\}$, and $\mathbf{F}(\mathbf{U}) = \{\mathbf{F}^f(\mathbf{U}), \mathbf{F}^m(\mathbf{U})\}$ with,

$$\begin{aligned}
\mathbf{U}^f &= \{\rho_i, \rho_i\vec{v}_i, E_i, \rho_e, \rho_e\vec{v}_e, E_e\}^\top \\
\mathbf{F}^f &= \{\rho_i v_i^x, \rho_i v_i^{x2} + p_i, \rho_i v_i^x v_i^y, \rho_i v_i^x v_i^z, (E_i + p_i)v_i^x, \\
&\quad \rho_e v_e^x, \rho_e v_e^{x2} + p_e, \rho_e v_e^x v_e^y, \rho_e v_e^x v_e^z, (E_e + p_e)v_e^x\}^\top \\
\mathbf{U}^m &= \{\vec{B}, \vec{E}, \phi, \psi\}^\top \\
\mathbf{F}^m &= \{\kappa\psi, -E^y, E^x, \xi\hat{c}^2\phi, \hat{c}^2 B^y, -\hat{c}^2 B^x, \xi E^x, \kappa\hat{c}^2 B^x\}^\top.
\end{aligned}$$

We exploit the split structure of the flux in (1.1) to design a four-wave HLL type approximate Riemann solver. Consider the Euler HLL speeds,

$$\begin{aligned}
b_l^f &= \min_j \min_\alpha(\lambda_j^\alpha(\mathbf{U}_i), \lambda_j^\alpha(\mathbf{U}_a), 0), \\
b_r^f &= \max_j \max_\alpha(\lambda_j^\alpha(\mathbf{U}_{i+1}), \lambda_j^\alpha(\mathbf{U}_a), 0),
\end{aligned}$$

with $\lambda_j^\alpha \in \{v_\alpha^x - c_\alpha, v_\alpha^x, v_\alpha^x + c_\alpha\}$, $\alpha \in \{i, e\}$, $c_\alpha = \sqrt{\gamma p_\alpha/\rho_\alpha}$ and the Maxwell HLL speeds $b_l^m = -\hat{c}$, $b_r^m = \hat{c}$. Here $\mathbf{U}_a$ represent the simple average of states $\mathbf{U}_i$ and $\mathbf{U}_{i+1}$. Then the four wave HLL type numerical flux for (1.1) is,

$$\mathbf{F}^{n,\beta}_{i+\frac{1}{2}} = \frac{b_r^\beta \mathbf{F}^\beta(\mathbf{U}_i^{n,\beta}) - b_l^\beta \mathbf{F}^\beta(\mathbf{U}_{i+1}^{n,\beta})}{b_r^\beta - b_l^\beta} + \frac{b_r^\beta b_l^\beta}{b_r^\beta - b_l^\beta}(\mathbf{U}_{i+1}^{n,\beta} - \mathbf{U}_i^{n,\beta}). \tag{2.4}$$

with $\beta \in \{f, m\}$.

2.2 Processing of source terms

Denote $\mathbf{U} = \{\mathbf{V}_1, \mathbf{V}_2, \mathbf{V}_3\}$ with,

$$\mathbf{V}_1 = \{\rho_i, \rho_e, B^x, B^y, B^z, \psi\}^\top$$

$$\mathbf{V}_2 = \{\rho_i v_i^x, \rho_i v_i^y, \rho_i v_i^z, \rho_e v_e^x, \rho_e v_e^y, \rho_e v_e^z, E^x, E^y, E^z\}^\top$$
$$\mathbf{V}_3 = \{E_i, E_e, \phi\}^\top$$

We observe that (2.1) can be rewritten in the following 3 blocks,

$$\mathbf{V}_{1,i}^{n+1} = \mathbf{G}_1(\mathbf{U}_{i-1}^n, \mathbf{U}_i^n, \mathbf{U}_{i+1}^n), \tag{2.5a}$$
$$\mathbf{V}_{2,i}^{n+1} = \mathbf{G}_2(\mathbf{U}_{i-1}^n, \mathbf{U}_i^n, \mathbf{U}_{i+1}^n) + \mathbb{A}(\mathbf{V}_{1,i}^n)\mathbf{V}_{2,i}^{n+1} \tag{2.5b}$$
$$\mathbf{V}_{3,i}^{n+1} = \mathbf{G}_3(\mathbf{U}_{i-1}^n, \mathbf{U}_i^n, \mathbf{U}_{i+1}^n) + \mathbf{H}(\mathbf{V}_{1,i}^{n+1}, \mathbf{V}_{2,i}^{n+1}). \tag{2.5c}$$

Here $\mathbf{G}_1, \mathbf{G}_2$ and $\mathbf{G}_3$ are the explicit flux updates using (2.1) of variables $\mathbf{V}_1, \mathbf{V}_2$ and $\mathbf{V}_3$ respectively. The Eqns. (2.5) are then solved in sequential manner:

I) Equation (2.5a) is updated explicitly as it involves the evaluation of terms at the previous time level.

II) Note that $\mathbb{A}(\mathbf{V}_{1,i}^{n+1})$ in Eqn. (2.5b) is,

$$\begin{bmatrix}
0 & \frac{B^{z,n+1}}{\hat{r}_g} & -\frac{B^{y,n+1}}{\hat{r}_g} & 0 & 0 & 0 & \frac{\rho_i^{n+1}}{\hat{r}_g} & 0 & 0 \\
-\frac{B^{z,n+1}}{\hat{r}_g} & 0 & \frac{B^{x,n+1}}{\hat{r}_g} & 0 & 0 & 0 & 0 & \frac{\rho_i^{n+1}}{\hat{r}_g} & 0 \\
\frac{B^{y,n+1}}{\hat{r}_g} & -\frac{B^{x,n+1}}{\hat{r}_g} & 0 & 0 & 0 & 0 & 0 & 0 & \frac{\rho_i^{n+1}}{\hat{r}_g} \\
0 & 0 & 0 & 0 & \frac{B^{z,n+1}}{\hat{r1}_g} & -\frac{B^{y,n+1}}{\hat{r}_{1g}} & \frac{\rho_e^{n+1}}{\hat{r}_{1g}} & 0 & 0 \\
0 & 0 & 0 & -\frac{B^{z,n+1}}{\hat{r}_{1g}} & 0 & \frac{B^{x,n+1}}{\hat{r}_{1g}} & 0 & \frac{\rho_e^{n+1}}{\hat{r}_{1g}} & 0 \\
0 & 0 & 0 & \frac{B^{y,n+1}}{\hat{r}_{1g}} & -\frac{B^{x,n+1}}{\hat{r}_{1g}} & 0 & 0 & 0 & \frac{\rho_e^{n+1}}{\hat{r}_{1g}} \\
\frac{-r_i}{K} & 0 & 0 & \frac{-r_e}{K} & 0 & 0 & 0 & 0 & 0 \\
0 & \frac{-r_i}{K} & 0 & 0 & \frac{-r_e}{K} & 0 & 0 & 0 & 0 \\
0 & 0 & \frac{-r_i}{K} & 0 & 0 & \frac{-r_e}{K} & 0 & 0 & 0
\end{bmatrix} \tag{2.6}$$

All the quantities in the matrix are already computed in step I. So, we can rewrite Eqn. (2.5b) as,

$$\mathbf{V}_{2,i}^{n+1} = \left(\mathbf{I} - (\Delta t)\mathbb{A}(\mathbf{V}_{1,i}^{n+1})\right)^{(-1)} (\mathbf{G}_2(\mathbf{U}_{i-1}^n, \mathbf{U}_i^n, \mathbf{U}_{i+1}^n)). \tag{2.7}$$

The term $\left(\mathbf{I} - (\Delta t)\mathbb{A}(\mathbf{V}_{1,i}^{n+1})\right)^{(-1)} (\mathbf{G}_2(\mathbf{U}_{i-1}^n, \mathbf{U}_i^n, \mathbf{U}_{i+1}^n))$ is evaluated symbolically. The Eqn. (2.5c) is now updated for $\mathbf{V}_3^{n+1}$ by evaluating $\mathbf{H}(\mathbf{V}_{1,i}^{n+1}, \mathbf{V}_{2,i}^{n+1})$.

III) High-order discretization: We use standard piecewise linear second order reconstruction using the minmod limiter (see [3]). High order (second and third order) time integration is achieved by using SSP-RK methods (see [5]), where each intermediate update is computed using the IMEX algorithm described above.

3 Numerical Results

In this section, we consider two benchmark test cases for illustrating the efficiency of the IMEX scheme (2.1) in approximating Eqns. (1.1). The first example is a generalization of the MHD Brio-Wu shock tube problem (see [1],[2]). The second example is a simulation of the soliton propagation in plasma flows (see [1]). For the comparison we use fully explicit schemes i.e. $\mathbf{S}(\mathbf{U}_i^{n+1})$ is replaced by $\mathbf{S}(\mathbf{U}_i^n)$ in (2.1).

3.1 Generalized shock tube Riemann problem

The initial conditions for the Riemann problem are,

$$\mathbf{U}_{\text{left}} = \begin{cases} \rho_i = 1.0 \\ p_i = 5 \times 10^{-5} \\ \rho_e = 1.0 \ m_e/m_i \\ p_e = 5 \times 10^{-5} \\ B^x = 0.75 \\ B^y = 1.0 \\ \vec{v}_i = \vec{v}_e = \vec{E} = 0 \\ \phi = \psi = B^z = 0 \end{cases} \qquad \mathbf{U}_{\text{right}} = \begin{cases} \rho_i = 0.125 \\ p_i = 5 \times 10^{-6} \\ \rho_e = 0.125 \ m_e/m_i \\ p_e = 5 \times 10^{-6} \\ B^x = 0.75 \\ B^y = -1.0 \\ \vec{v}_i = \vec{v}_e = \vec{E} = 0 \\ \phi = \psi = B^z = 0 \end{cases} \tag{3.1}$$

on a domain $(0, 1)$ with, $\mathbf{U} = \mathbf{U}_{\text{left}}$ for $x < 0.5$ and $\mathbf{U} = \mathbf{U}_{\text{right}}$ for $x > 0.5$. The electron-ion mass ratio is taken to be $m_i/m_e = 1832.6$. The problem is nondimensionalized using $p_0 = 10^{-4}$. Non-dimensional Debye length is taken to be 0.01. We compute solutions using two non-dimensional Larmor radii of 50 and 0.005. Neumann boundary conditions are used.

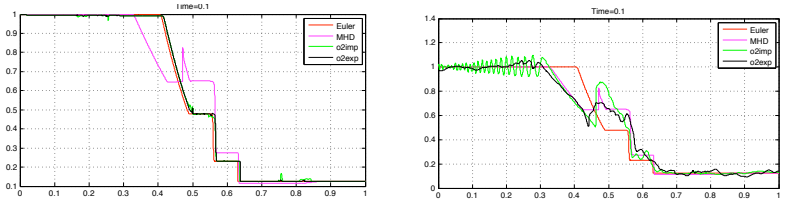

(a) Results with $\hat{r}_g = 50$. (b) Results with $\hat{r}_g = 0.005$.

Figure 3.1: Ion densities of Riemann problem (3.1) for o2exp and o2imp schemes with 20000 cells. Euler and MHD solutions are also plotted.

Results are presented in Fig. 3.1 using second order explicit scheme (o2exp) and second order IMEX scheme (o2imp) on a mesh with 20,000

cells. As expected, solutions with high Larmor radius of 50 (see Fig. 3.1(a)) are close to the Euler limit. In this case source terms are not stiff. Hence the time step is dictated by the convective CFL number, based on the maximum wave speed. The simulation time for o2exp is 16073.35 seconds and for o2imp it is marginally higher at 17482.41 seconds. For the lower Larmor radius of 0.005 solutions are close to the MHD solution. Also the o2imp solution has resolved all the dispersion effects whereas o2exp solution appears to be under resolved. In this case the source terms are stiff, hence the time step is dictated by the source terms. The simulation time for o2exp is 27377.6 sec and for o2imp it is 13613 sec. So the IMEX scheme is almost twice as fast compared to the fully explicit scheme.

3.2 Soliton Propagation

Initially the plasma is assumed to be stationary with ion density,

$$\rho_i = (1.0 + \exp(-25.0|x - L/3.0|)) \tag{3.2}$$

and mass ratio $m_i/m_e = 25$ on domain $D = (0, L)$ with $L = 12.0$. Electron pressure is $p_e = 5.0\rho_i$ with ion-electron pressure ratio of 1/100. Normalized Debye length is taken to be 1.0 and nomalized Larmor radius is 0.01. Periodic boundary conditions were used. Numerical results

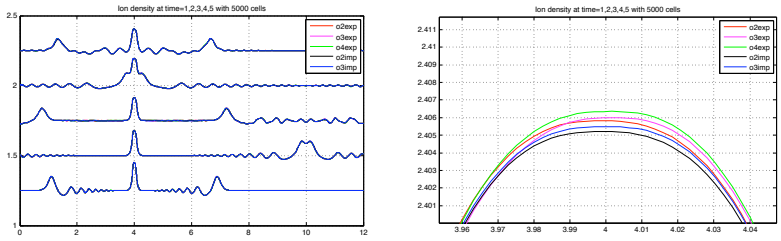

(a) Soliton propagation results plotted at time $t = 1, 2, 3, 4, 5$.

(b) Numerical solution at time $t = 5.0$ zoomed at middle stationary wave.

Figure 3.2: Ion densities for explicit schemes o2exp, o3exp, o4exp and implicit schemes o2imp, o3imp using 5000 cells.

are presented in fig. 3.2 using second (o2exp), third (o3exp), fourth (o4exp) order explicit time stepping and second (o2imp), third (o3imp) order IMEX schemes. In figure 3.2(a) we observe that all schemes perform comparably. However, when we zoom in the middle wave (see Fig. 3.2(b)), we observe that second (o2imp), third (o3imp) order IMEX schemes are slightly more diffusive compared to explicit schemes. Table 1 presents the simulation times for different schemes. In the case of low

resolution (No of cells less than 1000), time step is dictated by the source terms, so the IMEX schemes are faster. However, as we compute for finer resolutions the CFL condition dictates the time step, so simulation times of both schems are comparable.

Cells	o2exp	o3exp	o4exp	o2imp	o3imp
500	10.65	15.96	21.82	3.15	5.32
1000	21.25	31.52	44.09	12.36	18.58
2000	46.12	69.68	95.29	49.71	75.01
4000	185.05	277.53	396.77	200.46	299.41

Table 1: Simulation times for various schemes at different resolution.

4 Conclusion

We have presented finite volume based IMEX schemes for TF Eqns. (1.1). These schemes are then benchmarked using two numerical examples. These schemes are shown to be computationally faster than the fully explicit schemes on under resolved meshes.

References

[1] A. Hakim, J. Loverich and U. Shumlak. *A high-resolution wave-propagation scheme for ideal two-fluid plasma equations.* J. Comp. phys. 219 (2006), 418-442.

[2] U. Shumlak and J. Loverich. *Approximate Riemann solvers for the two-fluid plasma model.* J. Comp. Phys. 187 (2003), 620-638.

[3] R.J. LeVeque *Finite Volume Methods For Hyperbolic Problems* Cambridge University Press, Cambridge, 2002

[4] C. D. Munz, P. Omnes, R. Schneider, E. Sonnendru ker, U. Voβ *Divergence correction techniques for Maxwell solvers based on a hyperbolic model*, J. Comp. Phys. 161 (2000), 484-511.

[5] S. Gottlieb, C. W. Shu, E. Tadmor, *Strong stability-preserving high-order time discretization methods*, SIAM Rev., 43 (2001), 89-112.

Research Reports

No.	Authors/Title
10-29	*H. Kumar* Finite volume methods for the two-fluid MHD equations
10-28	*S. Kurz and H. Heumann* Transmission conditions in pre-metric electrodynamics
10-27	*F.G. Fuchs, A.D. McMurry, S. Mishra and K. Waagan* Well-balanced high resolution finite volume schemes for the simulation of wave propagation in three-dimensional non-isothermal stratified magneto-atmospheres
10-26	*U.S. Fjordholm, S. Mishra and E. Tadmor* Well-balanced, energy stable schemes for the shallow water equations with varying topography
10-25	*U.S. Fjordholm and S. Mishra* Accurate numerical discretizations of non-conservative hyperbolic systems
10-24	*S. Mishra and Ch. Schwab* Sparse tensor multi-level Monte Carlo finite volume methods for hyperbolic conservation laws with random intitial data
10-23	*J. Li, J. Xie and J. Zou* An adaptive finite element method for distributed heat flux reconstruction
10-22	*D. Kressner* Bivariate matrix functions
10-21	*C. Jerez-Hanckes and J.-C. Nédélec* Variational forms for the inverses of integral logarithmic operators over an interval
10-20	*R. Andreev* Space-time wavelet FEM for parabolic equations
10-19	*V.H. Hoang and C. Schwab* Regularity and generalized polynomial chaos approximation of parametric and random 2nd order hyperbolic partial differential equations
10-18	*A. Barth, C. Schwab and N. Zollinger* Multi-Level Monte Carlo Finite Element method for elliptic PDE's with stochastic coefficients
10-17	*B. Kågström, L. Karlsson and D. Kressner* Computing codimensions and generic canonical forms for generalized matrix products